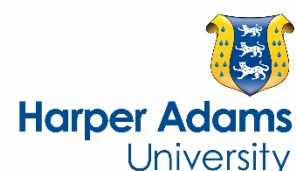# Natural evolution of alkaline characteristics in bauxite residue

by Kong, X., Guo, Y., Xue, S., Hartley, W., Wu, C., Ye, Y. and Cheng, Q.

Harper Adams University

Natural evolution of alkaline characteristics in bauxite residue

Xiangfeng Kong [a, b], Yiwei, Li [a, b], Shengguo Xue [a, b, *], William Hartley [c], Xiaofei Li [a, b],

Jiaxin Liao [a, b]

[a] School of Metallurgy and Environment, Central South University, 932 Lushan South Road, Changsha, Hunan, 410083, PR China

[b] Chinese National Engineering Research Center for Control & Treatment of Heavy Metal Pollution, Central South University, Changsha, 410083, PR China

[c] Crop and Environment Sciences Department, Harper Adams University, Newport, Shropshire, TF10 8NB, United Kingdom[1]

Abstract: Bauxite residue, a highly alkaline solid waste, is extremely hazardous to the surrounding environment and current research approaches have largely focused on the removal and separation of alkaline substances. Natural weathering processes may be a step forward in terms of their regeneration. In this study, natural evolution of basic alkalinity, electrical conductivity, exchangeable ions and acid neutralizing capacity of residue in the disposal areas is discussed. Minerals, exchangeable cations and alkaline anions were analyzed by X-ray powder diffraction (XRD), inductively coupled plasma atomic emission spectroscopy (ICP-AES) and titration, respectively. Acid neutralizing capacity was carried out by batch neutralization experiments. Basic alkalinity, electrical conductivity, cation exchange capacity and exchangeable sodium percentage decreased with increasing disposal duration. Sodium was the predominant exchangeable cation in fresh residue but its concentration significantly decreased with increasing time from initial disposal. The acid neutralizing capacity of bauxite residue was investigated by incubation with hydrochloric acid. Acid neutralizing capacity curves changed with disposal duration and each revealed a characteristic buffering behavior that could be controlled by its alkaline components.

*Corresponding author. Tel: + 86 731 85552958

E-mail address: sgxue70@hotmail.com (S.G. Xue); sgxue@csu.edu.cn

1. Introduction

As a result of the high demand for aluminum, the global alumina industry has developed rapidly. However, these rapid developments have triggered numerous environmental issues (Gelencser et al., 2011; Mayes et al., 2016; Ruyters et al., 2011) that severely restrict the sustainable development of the alumina industry. Bauxite residue (red mud) is an alkaline solid waste generated by extraction of alumina from bauxite in refineries. The volume of bauxite residue generated while producing one ton of alumina is typically about 0.5-2 tons. With increasing demand for alumina worldwide, the global inventory of bauxite residue has reached an estimated 4 billion tons based on its current rate of production, and is still rapidly increasing (Kinnarinen et al., 2015; Liu and Naidu, 2014; Power et al., 2011). China is the largest producer of alumina in the world (Liu et al., 2014; Si et al., 2013). Its accumulative inventory of bauxite residue has reached over an estimated 0.6 billion tons with an annual increase of more than 70 million tons (Xue et al., 2016). Currently, almost all bauxite residue is stored indefinitely in land-based bauxite residue disposal areas (BRDAs) (Burke et al., 2013; Santini et al., 2015; Zhu et al., 2016a), which require continuous resources to manage and transform the waste and reduce its potential to contaminate water and land, as well as the surrounding ecology (Banning et al., 2014; Lockwood et al., 2015; Santini and Fey, 2015). Leaching of alkaline waste is a further potential problem (Buckley et al., 2016; Pulford et al., 2012; Samal et al., 2015). The adverse alkalinity means that bauxite residue is listed as a contaminated waste, which limits its disposal, applications and options for its sustainable reuse.

Many amelioration techniques have been developed in an attempt to reduce the alkalinity of bauxite residue. For example, seawater neutralization is used by some coastal refineries (e.g. Shandong Aluminium Industry Co., Ltd; Queensland Alumina), which involves the addition of excess seawater to convert soluble hydroxides, aluminates and carbonates into insoluble solids as calcite ($CaCO_3$), hydrocalumite

56 $(Ca_4Al_2(OH)_{12}\cdot CO_3)$, aluminohydrocalcite $(CaAl_2(CO_3)_2(OH)_4\cdot 3H_2O)$, brucite

57 $(Mg_3(OH)_6)$ and hydrotalcite $(Mg_6Al_2(CO_3)(OH)_{16}\cdot 4H_2O)$ (Clark et al., 2015; Johnston

58 et al., 2010; Menzies et al., 2004). Seawater neutralization lowers pH and alkalinity, but

59 the generated colloidal particles are difficult to deal with. Carbon dioxide (CO_2)

60 sequestration utilizes the reaction of CO_2 with OH^- to form HCO_3^-, and the reversibility

61 of key alkalinity reactions between OH^-, CO_3^{2-} and HCO_3^- (Renforth et al., 2012; Wang

62 et al., 2009; Yadav et al., 2010). The innovative nature of this technique is the

63 consumption of CO_2 to reduce atmospheric and industrial carbon dioxide emissions via

64 sequestration (Cooling et al., 2002; Guilfoyle et al., 2005; Rai et al., 2013; Sahu et al.,

65 2010). Interaction of waste acid can react with and transform hydroxides, oxides and

66 sodalite (Freire et al., 2012; Lu et al., 2010), but the leached liquor and residue becomes

67 a complex problem to manage, generating additional pollution issues (Burke et al., 2013;

68 Goloran et al., 2015; Zhu et al., 2015a). Furthermore, the physical properties of

69 bauxite residue present a problem, being a hostile environment for plant establishment

70 (Borra et al., 2015; Kopittke, 2004; Zhu et al., 2015b). Gypsum transformation of

71 bauxite residue lowers the pH by precipitating OH^-, $Al(OH)_4^-$, and CO_3^{2-} as calcium

72 hydroxide $(Ca(OH)_2)$, tri-calcium aluminate (TCA, $Ca_3Al_2(OH)_{12}$), hydrocalumite

73 $(Ca_4Al_2(OH)_{12}\cdot CO_3)$ and calcite $(CaCO_3)$ (Babu and Reddy, 2011; Courtney and

74 Kirwan, 2012). The efficacy of gypsum in transforming the alkalinity is limited to

75 gypsum's ability to readily dissolve (Courtney et al., 2009; Courtney and Harrington,

76 2012).

77 These amelioration strategies may temporarily contribute to reduce the alkalinity of

78 bauxite residue, but nevertheless there remains insufficient long-term success due to

79 side effects and economic issues. Many of the current research techniques have focused

80 on artificial amelioration of alkaline substances with less attention being paid to the

81 natural evolution of alkalinity and its occurrence in bauxite residue.

82 There is limited mechanistic understanding of bauxite residue alkalinity

83 characteristics following its long term disposal. Indeed, lack of understanding of

84 evolution chemistry and alkalinity behavior has been highlighted as a significant

85 knowledge gap in relation to the safe management and revegetation of bauxite residue

86   in BRDAs. This study therefore had the following specific objectives: (1) Discuss the

87   changes in overall alkalinity of bauxite residue during its disposal history. (2) Identify

88   the quantitative relationships between EC, Na^+ and OH^-. (3) Investigate the

89   transformations in exchangeable cation and sodium percentages. (4) Understand the

90   neutralization behavior following long term natural evolution of the residue.

91   **2. Materials and methods**

92   *2.1 Field sampling and sample handling*

93   The raw bauxite residue sample used in this study was collected at the BRDA of the

94   Zhongzhou refinery, Aluminum Corporation of China, Henan province, China.

95   Samples were collected from 5 locations as follows; freshly deposited residue (0 years)

96   (Lat 35°24′3.76″ N, Long 113°25′38.18″ E), 5 year old residue (5) (Lat 35°24′3.03″ N,

97   Long 113°25′38.82″ E), 10 year old residue (10) (Lat 35°24′2.43″ N, Long

98   113°25′38.26″ E), 15 year old residue (15) (Lat 35°24′1.86″ N, Long 113°25′40.39″ E)

99   and 20 year old residue (20) (Lat 35°24′28.11″ N, Long 113°25′47.33″ E).   Residue

100   age differences are approximate but were determined due to a change in zonation which

101   was clearly visible within the stacks. At each location, three sub-samples were collected

102   with a distance of 5 meters from each other to form a representative sample. Samples

103   were stored in polyethylene bags, returned to the laboratory and subsequently air-dried

104   for 1 week, disaggregated using a mortar and pestle, and sieved to retain the <2 mm

105   fraction. Subsequently, X-ray powder diffraction (XRD) analysis was conducted on the

106   samples using a Bruker D8 discover 2500 with a Cu Ka_1 tube using a Sol-X detector.

107   X-ray diffraction patterns were collected from 10 to 80° at a scan rate of 1° 2θ /min and

108   a step size of 0.04° 2θ. XRD data analysis used the PANalytical analysis package to

109   identify and quantify phases.

110   *2.2 Analytical methods*

111   Bauxite residue : water (1:5) extracts were prepared to determine pH, electrical

112   conductivity (EC), and alkaline anions, and a bauxite residue : 1mol/L ammonium

113   acetate (1:5) extract was prepared to analyze exchangeable cations. Supernatant liquors

from the water extraction were mixed at 150 rpm (1 h) then centrifuged at 3000 rpm

(10 min) and analyzed for pH and EC (Clark et al., 2015). Sodium, K, Ca and Mg in

ammonium acetate (pH=7) extracts were analyzed by inductively coupled plasma

atomic emission spectroscopy (ICP-AES). Since no exchangeable acidic cations are

expected to exist in alkaline conditions, the sum of exchangeable Na, K, Ca and Mg

can be used as an estimate of cation exchange capacity (CEC).

Prepared supernatants from the water extraction were analyzed for alkaline anions

(carbonate, bicarbonate and aluminate) by titration using a 0.02 mol/L H_2SO_4

standardized solution. The supernatant (5 mL) was diluted with Milli-Q water to 30 ml.

For solutions that were initially at a pH above 10.5, the solution was titrated to pH 10.3

(first titration), and then a 250 g/L sodium gluconate solution was added until pH no

longer increased. The solution was then titrated from pH 10.3 (second titration) to pH

4.5 (third titration) (Kirwan et al., 2013). For solutions that were initially at a pH

between 8.3 and 10.3, the solution was directly titrated to pH 4.5 (third titration). From

the first titration, the free hydroxide concentration (OH^-) was determined. From the

second titration, the aluminate concentration ($Al(OH_4)^-$) was determined, and from the

third titration, the carbonate concentration (CO_3^{2-}) was measured.

2.3 Batch neutralization experiments

Acid neutralizing capacity (ANC) from each of the 5 locations was determined by

repeatedly titrating the supernatants. Samples (10 g) were weighed into conical flasks

(100 ml). Hydrochloric acid (HCl) (0.5 mol/L) was subsequently added at 0.8 ml

increments, and made up to volume (50 ml) with Milli-Q water. The supernatant liquors

were then shaken by hand and pH determined immediately. Samples were then placed

on a shaker operating at 120 rpm (25°C). Supernatant pH was determined after 1 min,

then on day 1, 5, 15, 30 and 60 of shaking. Measurements were conducted on

supernatants in the conical flasks without removal of any sample. All samples (each in

duplicate) from the different disposal dates were used for ANC determinations.

3. Result and discussion

3.1 Transformation of basic alkalinity

Basic alkalinity of the residue from the five locations are presented in Table 1. Following disposal, alkalinity decreased. For fresh residue, initial alkalinity was 28349.69 mg/L Na_2CO_3, compared to 21857.02 mg/L Na_2CO_3 from the 20 year old disposal area. Alkalinity is a result of the caustic solution from the Bayer process, and because of incomplete washing prior to disposal, alkaline substances (sodium hydroxide, $NaOH$; sodium carbonate, Na_2CO_3; sodium aluminate, $NaAl(OH)_4$) remain in the bauxite residue. During disposal, compounds such as OH^-, CO_3^{2-}, and $Al(OH)_4^-$, will undergo a chemical transformation. These reactions are expressed as Eqs. (1), (2) and (3). Notably, the concentration of OH^- was greatly reduced after 15 years following disposal.

$$OH^- + H^+ \rightarrow H_2O \tag{1}$$
$$CO_3^{2-} + H^+ \rightarrow HCO_3^- \tag{2}$$
$$Al(OH)_4^- + H^+ \rightarrow Al(OH)_3 + H_2O \tag{3}$$

Slaked lime ($Ca(OH)_2$) is commonly added within the Bayer process to improve digestion of alumina from the ore. This can lead to the formation of many solid phase calcium hydroxides, carbonates and aluminates, such as hydrogarnet ($Ca_3Al_2(SiO_4)_x(OH)_{12-4x}$), calcite ($CaCO_3$) and tri-calcium aluminate (TCA, $Ca_3Al_2(OH)_{12}$) (Fig. 1). These insoluble solids act as an alkali store and their dissolution (hydrogarnet, Eq. (4); calcite, Eq. (5); tri-calcium aluminate, Eq. (6)) can provide a continuous source of alkaline compounds OH^-, CO_3^{2-} and $Al(OH)_4^-$ (Gomes et al., 2015). These alkaline anions are continuously consumed (Fig. 1), but even after 20 years, the alkalinity of the residue remained at a relatively high level; this may be attributed to these insoluble solid substances.

$$Ca_3Al_2(SiO_4)_x(OH)_{12-4x} \rightarrow (6-4x)OH^- \tag{4}$$

$$+3Ca^{2+}+2Al(OH)_3+xH_4SiO_4$$

$$CaCO_3 \rightarrow Ca^{2+}+CO_3^{2-} \tag{5}$$

$$Ca_3Al_2(OH)_{12} \rightarrow 6OH^-+3Ca^{2+}+2Al(OH)_3 \tag{6}$$
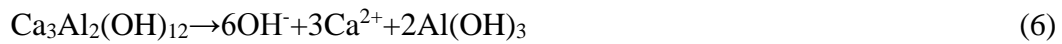
166

167   The de-silication products (DSPs) are a sub-set of more general Bayer process

168   characteristic solids (BPCSs) generated by the reaction of reactive silica with sodium

169   hydroxide and which impart significant alkalinity to the residues. The main DSPs

170   formed are Bayer sodalite ($[Na_6Al_6Si_6O_{24}] \cdot [2NaOH$ or $Na_2CO_3]$) and cancrinite

171   ($[Na_6Al_6Si_6O_{24}] \cdot 2[CaCO_3]$) (Fig. 1); they have a zeolite-type caged construction which

172   can attach sodium. These anions tend to be dominated by OH^-, CO_3^{2-}, and $Al(OH)_4^-$.

173   With natural disposal, it is difficult for these attached anions to be released and

174   transformed. Hence in this way, DSPs can be a source of alkalinity. The natural

175   transformation of these anions associated with the dissolution of DSP results in

176   relatively stable alkalinity. However, with increasing duration following disposal,

177   concentration of sodalite, hydrogarnet and calcite (Fig. 1) gradually reduced, whilst free

178   hydroxides, carbonates and aluminates changed and the alkaline nature of the residue

179   decreased.

180   *3.2 Transformation of electrical conductivity*

181   During disposal, EC decreased with increasing duration following disposal (Fig. 2).

182   For fresh residue, the initial EC was 3.73 mS/cm, compared to 0.36 in the 20 year old

183   residue. During disposal, electrical conductivity affected the evolution of the residues

184   alkaline characteristics. To elucidate the relationships between EC and alkaline sodium

185   ions (Na^+) and EC and hydroxide ions (OH^-)   linear curves were plotted (Fig. 3 and

186   Fig. 4). High EC values present high concentrations of alkaline Na^+ and is replenished

187   from Na-bearing solids. With increasing time from initial disposal, Na-bearing solids

188   decreased with a corresponding decrease in EC (Fig. 2).

189   Electrical conductivity is also related to hydroxide ions (OH^-), and it is important to

190   note that the linear relationship is approximately a factor of 1/3. The linear curve was a

191   good fit and showed EC (mS/cm) ~ 1/3 OH^- (mmol/L) (Fig. 4). High EC values also

192 demonstrate high concentrations of OH$^-$. The dissolution reactions are the main source

193 of OH$^-$, which result in bauxite residue becoming weakly alkaline with increasing
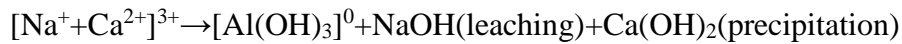
194 duration following disposal.

195 In the absence of detailed supernatant compositional data, EC is the most feasible

196 quantity to estimate ionic strength. In natural aqueous solutions, Griffin and Jurinak

197 (1973) determined the equation of EC ~ 78 IS. The double-layer thickness of charged

198 particles of bauxite residue becomes weak. Residue particles become dispersed, and the

199 osmotic potential becomes more favorable. These transformed properties are beneficial

200 to the disposal of bauxite residue and to stabilize the BRDA over the long term.

201 *3.3 Transformation of exchangeable cations*

202 The natural evolution of exchangeable cations (Na, K, Ca, Mg) are presented in Fig.

203 5. Exchangeable Na decreased with increasing disposal time whilst exchangeable K,

204 Ca and Mg increased with increasing time following disposal. For fresh bauxite residue,

205 the molar concentrations of various exchangeable cations were in the following

206 decreasing order: Na > Ca > Mg > K. Exchangeable Na accounted for approximately

207 72 % of the total exchangeable cations (mean molar concentration). This revealed that

208 exchangeable Na dominated the basic cations in fresh bauxite residue. However, the

209 concentration of exchangeable Na decreased from 20.28 cmol$_c$/kg in fresh residue to

210 9.81 cmol$_c$/kg in 20 year old residue. The concentration of exchangeable Ca increased

211 from 6.96 cmol$_c$/kg in fresh residue to 17.40 cmol$_c$/kg in 20 year old residue. The

212 increase in K and Mg was however not obvious, indicating that a large concentration

213 of exchangeable Na was replaced with exchangeable Ca during the disposal process.

214 It should also be noted that the cation exchange capacity (CEC) of the residue

215 decreased with increasing duration following disposal (Fig. 6). This may be attributed

216 to a reduction in pH over time (Eq.(7), resulting in precipitation of Ca(OH)$_2$ but also

217 leaching of NaOH. The original negatively charged [Al(OH)$_6$]$^{3-}$ lost three OH$^-$ which

218 resulted in zero-charged [Al(OH)$_3$]^0 (Eq. (8)). Similar exchange reactions are available

219 at edge sites of other alkaline compounds. The charged state of the colloids is therefore

220 a significant regulator for cation exchange. During the time from disposal, with a

221   reduction in CEC, the negatively charged sites became increasingly positive.
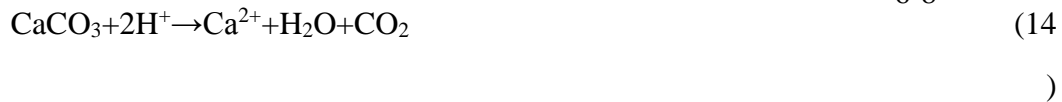
$$[Al(OH)_6]^{3-} \tag{7}$$

$$[Na^+ + Ca^{2+}]^{3+} \rightarrow [Al(OH)_3]^0 + NaOH(leaching) + Ca(OH)_2(precipitation)$$

$$[Al(OH)_6]^{3-} - 3OH^- \rightarrow zero\text{-}charged\ [Al(OH)_3]^0 \tag{8}$$
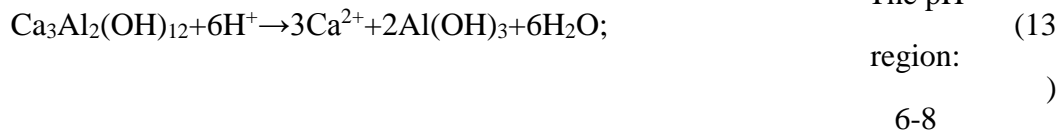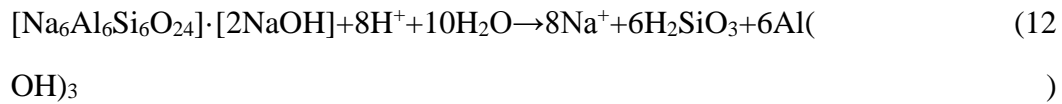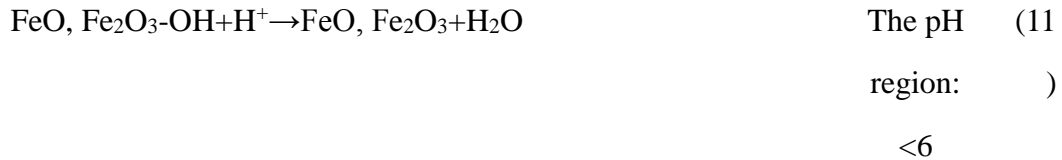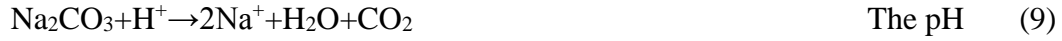
222   The exchangeable sodium percentage (ESP) (Fig. 7) decreased with increasing

223 duration following disposal. The ESP approximates to the composition of cation

224 exchange sites on the residue surface as a result of the composition of exchangeable Na,

225 Ca and Mg (Gräfe and Klauber, 2011). Sodium ions can't be dehydrated as readily as

226 Ca and Mg, which is indicative of stable hydration layers in bauxite residue particles.

227 Additionally, Na ions can't be coordinated with negatively charged surfaces. The effect

228 is that particles of fresh bauxite residue do not aggregate well and usually tend to be

229 crusted and eroded in the dry state as Na eventually precipitates out as soda ash (trona

230 and nahcolite), which simultaneously leads to the formation of alkaline dust and

231 efflorescence at the surface of BRDAs (Klauber et al., 2008). The poor structural

232 conditions at the surface of BRDAs are ultimately dependent on revegetation. With

233 increasing time following disposal, the poor structural conditions may gradually be

234 ameliorated (Zhu et al., 2016b).

235 *3.4 Transformation of Acid neutralizing capacity*

236   Acid neutralization of fresh residue shows changes in pH created by addition of

237 hydrochloric acid (Fig. 8). Acid neutralizing capacity (ANC, final pH 7) of 1 min, 1, 5,

238 15, 30 and 60 days were 0.091 mol H^+/kg, 0.27 H^+/kg, 0.36 H^+/kg, 0.57 H^+/kg, 0.68

239 H^+/kg and 0.78 H^+/kg solids, respectively. Fig. 8 shows that the moles of H^+ taken to

240 reach pH 7 increase as neutralizing time elapses, and most of the increase occurs at day

241 1 and 5. The curve at day 60 reveals an extensive horizontal section. Some of this

242 neutralizing behavior can be attributed to soluble free Na_2CO_3 and NaOH (Eqs. (9) and

243 (10)) occurring at the region of pH>8. Much of this neutralizing behavior is associated

244 with hydroxyls on the surfaces of iron oxides (FeO, Fe_2O_3-OH, its reaction (Eq. (11)

245 occurs at the region of pH<6) in the bauxite residue and dissolution of sodalite,

246 tricalcium aluminate and calcite ($[Na_6Al_6Si_6O_{24}] \cdot [2NaOH]$, $Ca_3Al_2(OH)_{12}$ and $CaCO_3$

247 (Eqs. (12), (13) and (14) (Snars and Gilkes, 2009; Wissmeier et al., 2011; Xue et al.,

248 2016). The length of the neutralizing region reflects the contents of these components

249 in the bauxite residue.

$$Na_2CO_3+H^+\rightarrow 2Na^++H_2O+CO_2 \qquad \text{The pH} \qquad (9)$$

$$NaOH+H^+\rightarrow Na^++H_2O \qquad \text{region: >} \qquad (10)$$

$$8$$

$$FeO, Fe_2O_3\text{-}OH+H^+\rightarrow FeO, Fe_2O_3+H_2O \qquad \text{The pH} \qquad (11)$$

$$\text{region:}$$

$$<6$$

$$[Na_6Al_6Si_6O_{24}]\cdot[2NaOH]+8H^++10H_2O\rightarrow 8Na^++6H_2SiO_3+6Al(OH)_3 \qquad (12)$$

$$Ca_3Al_2(OH)_{12}+6H^+\rightarrow 3Ca^{2+}+2Al(OH)_3+6H_2O; \qquad \text{The pH} \qquad (13)$$

$$\text{region:}$$

$$6\text{-}8$$

$$CaCO_3+2H^+\rightarrow Ca^{2+}+H_2O+CO_2 \qquad (14)$$

250 The natural evolution of acid neutralizing capacity (ANC) (Fig. 9) was examined due

251 to the characteristics of the fresh bauxite residue (Fig. 8). During disposal, ANC

252 demonstrated some inconsistencies with increasing duration following disposal. For

253 fresh residue, the initial ANC recorded (at pH 7) was 0.78 mol H^+/kg solid, which

254 presents a strong ANC compared to 0.25 mol H^+/kg solid from the 20 year old residue.

255 The ANC of fresh residue was higher than that of the residue disposed over the long

256 term, which may be attributed to partial removal of NaOH and Na_2CO_3 by leaching

257 during rainfall and alkali compound transformations. Furthermore, the curves for fresh

258 and 5 year old residue (Fig. 9) present a broad horizontal section; the curves for 10, 15

259 and 20 year old residue (Fig. 9) only exhibit a narrow section. This neutralizing

260 behavior is associated with the dissolution of sodalite, tricalcium aluminate, calcite and

261 other alkaline compounds (Snars and Gilkes, 2009; Wissmeier et al., 2011). This

262 tendency may demonstrate that fresh bauxite residue contains a larger concentration of

263 sodalite, tricalcium aluminate and calcite, compared to aged residues (consistent with

264 Fig.1 results). Further, the acid neutralizing behavior may enhance the natural evolution

265   of alkaline substances in bauxite reside following disposal.

266   *3.5 Environmental management for long-term disposal*

267   Historically, the management practices of BRDAs have focused on containment,

268   with little attention given to long term changes in the chemical and physical properties

269   of the residues. Currently, management plans are moving towards remediation and

270   revegetation and/or further soil-formation of BRDAs to reduce environmental risks

271   associated with long term disposal. Subsequently this will establish a stable

272   ecosystem in the residue disposal areas, finally returning occupied land areas to an

273   alternative option. In this work, alkalinity of bauxite residue was reduced with

274   increasing duration following disposal. In addition, aged residue particles (10 to 20

275   years) had favorable osmotic potential that can't be considered dangerous to the

276   surrounding environment and may be safely disposed. Furthermore, the long-term

277   disposal of bauxite residue allows a significant decrease in exchangeable Na, EC, and

278   pH values, which can increase the rate of revegetation. The ecological restoration of

279   bauxite residue has many challenges due to its high alkalinity, salinity and sodium

280   content, deficiencies in organic matter and nutrient concentrations. Recent research has

281   indicated the possibility for surface revegetation by Bermuda grass (*Cynodon dactylon*)

282   together with arbuscular mycorrhizal fungi (Babu and Reddy, 2011) and giant reed

283   (*Arundo donax L.*) (Alshaal et al., 2013). Revegetation of bauxite residue following

284   disposal in combination with phytoremediation may be a feasible option in the future.

285   Recently disposed bauxite residue presents potential threats to the environment

286   such as leakage of alkaline compounds into groundwater, risk of caustic exposure to

287   organisms, overflow of alkaline substances during storm events and the loss of alkaline

288   dust and efflorescence forming at the surface of BRDAs, which require sustained and

289   intensive resources to manage and transform their alkalinity. Several methods have

290   been considered for safe disposal, including washing, dewatering, covering with

291   vegetation, neutralization and wetland construction (Burke et al., 2013; Liu et al., 2014;

292   Santini and Banning, 2016). It is critical that residues are washed and dewatered for

293   separation of caustic liquors prior to disposal into BRDAs. Following this, the residue

294 particles may aggregate well and be stable rather than crusted and become eroded.
295 Furthermore, the formation of alkaline dust and efflorescence at the residue surface may
296 be ameliorated and the residue may be safely stored for long-term natural regeneration.

297 **4. Conclusion**

298 This work provides evidence for the natural evolution of alkaline characteristics of
299 bauxite residue in BRDAs following long term disposal. Bauxite residue has highly
300 alkaline characteristics which decrease with increasing duration following disposal.
301 High EC is related to Na^+ and OH^- which appear to decrease with increasing disposal
302 time. Cation exchange capacity and exchangeable sodium percentage decrease with
303 increasing duration following disposal. Furthermore, Na was the predominant
304 exchangeable cation in fresh residue but decreased over the long term being replaced
305 with Ca. Acid neutralizing capacity curves changed with disposal history and bauxite
306 residue demonstrated a characteristic buffering behavior that further confirms the
307 natural evolution of alkalinity. More importantly, these findings are applicable to
308 surface revegetation and improved soil-formation because they demonstrate that
309 decreasing alkalinity and increasing structural formation have a positive influence on
310 the residues physical and chemical properties.

Reference

Alshaal T., Domokos-Szabolcsy E., Marton L., Czako M., Katai J., Balogh P., Elhawat N., El-Ramady H., Fari M., 2013. Phytoremediation of bauxite-derived red mud by giant reed. Environ. Chem. Lett. 11, 295-302. http://dx.doi.org/10.1007/s10311-013-0406-6.

Babu A.G., Reddy M.S., 2011. Influence of arbuscular mycorrhizal fungi on the growth and nutrient status of bermudagrass grown in alkaline bauxite processing residue. Environ. Pollut. 159, 25-29. http://dx.doi.org/10.1016/j.envpol.2010.09.032.

Banning N.C., Sawada Y., Phillips I.R., Murphy D.V., 2014. Amendment of bauxite residue sand can alleviate constraints to plant establishment and nutrient cycling capacity in a water-limited environment. Ecol. Eng. 62, 179-187. http://dx.doi.org/10.1016/j.ecoleng.2013.10.034.

Borra C.R., Pontikes Y., Binnemans K., Van Gerven T., 2015. Leaching of rare earths from bauxite residue (red mud). Miner. Eng. 76, 20-27. http://dx.doi.org/10.1016/j.mineng.2015.01.005.

Buckley R., Curtin T., Courtney R., 2016. The potential for constructed wetlands to treat alkaline bauxite residue leachate: Laboratory investigations. Environ. Sci. Pollut. Res. 23, 14115-14122. http://dx.doi.org/10.1007/s11356-016-6582-8.

Burke I.T., Peacock C.L., Lockwood C.L., Stewart D.I., Mortimer R.J.G., Ward M.B., Renforth P., Gruiz K., Mayes W.M., 2013. Behavior of aluminum, arsenic, and vanadium during the neutralization of red mud leachate by HCl, gypsum, or seawater. Environ. Sci. Technol. 12, 6527-6535. http://dx.doi.org/10.1021/es4010834.

Clark M.W., Johnston M., Reichelt-Brushett A.J., 2015. Comparison of several different neutralisations to a bauxite refinery residue: Potential effectiveness environmental ameliorants. Appl. Geochem. 56, 1-10. http://dx.doi.org/10.1016/j.apgeochem.2015.01.015.

Cooling D.J., Hay P.S., Guifoyle L., 2002. Carbonation of bauxite residue. Proceedings of the 6th International Alumina Quality Workshop, Brisbane.

Courtney R., Harrington T., 2012. Growth and nutrition of Holcus lanatus in bauxite residue amended with combinations of spent mushroom compost and gypsum. Land Degrad. Dev. 23, 144-149. http://dx.doi.org/10.1002/ldr.1062.

Courtney R., Kirwan L., 2012. Gypsum amendment of alkaline bauxite residue - Plant available aluminium and implications for grassland restoration. Ecol. Eng. 42, 279-282. http://dx.doi.org/ 10.1016/j.ecoleng.2012.02.025.

Courtney R.G., Jordan S.N., Harrington T., 2009. Physico-chemical changes in bauxite residue following application of spent mushroom compost and gypsum. Land Degrad. Dev. 20, 572-581. http://dx. doi.org/10.1002/ldr.926.

Freire T.S.S., Clark M.W., Comarmond M.J., Payne T.E., Reichelt-Brushett A.J., Thorogood G.J., 2012. Electroacoustic isoelectric point determinations of bauxite refinery residues: Different neutralization techniques and minor mineral effects.

360   Langmuir. 28, 11802-11811. http://dx.doi.org/ 10.1021/la301790v.

361 Gelencser A., Kovats N., Turoczi B., Rostasi A., Hoffer A., Imre K., et al., 2011. The
362   red mud accident in ajka (Hungary): Characterization and potential health effects
363   of fugitive dust. Environ. Sci. Technol. 45, 1608-1615.
364   http://dx.doi.org/10.1021/es104005r.

365 Goloran J.B., Phillips I.R., Condron L.M., Chen C., 2015. Shifts in leaf nitrogen to
366   phosphorus ratio of Lolium rigidum grown in highly alkaline bauxite-processing
367   residue sand with differing age of rehabilitation and amendments. Ecol. Indic. 57,
368   32-40. http://dx.doi.org/10.1016/j.ecolind.2015. 04.018.

369 Gomes H.I., Mayes W.M., Rogerson M., Stewart D.I., Burke I.T., 2015. Alkaline
370   residues and the environment: A review of impacts, management practices and
371   opportunities. J. Clean. Prod. http://dx.doi.org/10.1016/j.jclepro.2015.09.111.

372 Gräfe M., Klauber C., 2011. Bauxite residue issues: IV. Old obstacles and new
373   pathways for in situ residue bioremediation. Hydrometallurgy. 108, 46-59.
374   http://dx.doi.org/10.1016/j.hydromet.2011. 02.005.

375 Guilfoyle L., Hay P., Cooling D., 2005. Use of flue gas for carbonation of bauxite
376   residue. Proceedings of the 7th International Alumina Guality Workshop, Perth,
377   Australia.

378 Johnston M., Clark M.W., McMahon P., Ward N., 2010. Alkalinity conversion of
379   bauxite refinery residues by neutralization. J. Hazard. Mater. 182, 710-715.
380   http://dx.doi.org/10.1016/j.jhazmat. 2010.06.091.

381 Kinnarinen T., Lubieniecki B., Holliday L., Helsto J., Häkkinen A., 2015. Recovery of
382   sodium from bauxite residue by pressure filtration and cake washing. Int. J. Miner.
383   Process. 141, 20-26. http://dx.doi.org/10.1016/j.minpro.2015.06.006.

384 Kirwan L.J., Hartshorn A., McMonagle J.B., Fleming L., Funnell D., 2013. Chemistry
385   of bauxite residue neutralisation and aspects to implementation. Int. J. Miner.
386   Process. 119, 40-50. http://dx.doi.org/ 10.1016/j.minpro.2013.01.001.

387 Klauber C., Harwood N., Hockridge R., Middleton C., 2008. Proposed mechanism for
388   the formation of dust horizons on bauxite residue disposal area. TMS Light Metals.
389   1, 19-24. http://dx.doi.org/ 10.1002/9781118647868.ch132.

390 Kopittke P.M., 2004. Limitations to plant root growth in highly saline and alkaline
391   bauxite residue. J. Bio. Chem. 277, 44651-9.

392 Liu W., Chen X., Li W., Yu Y., Yan K., 2014. Environmental assessment, management
393   and utilization of red mud in China. J. Clean. Prod. 84, 606-610.
394   http://dx.doi.org/10.1016/j.jclepro.2014.06.080.

395 Liu Y., Naidu R., 2014. Hidden values in bauxite residue (red mud): Recovery of metals.
396   Waste Manage. 34, 2662-2673. http://dx.doi.org/10.1016/j.wasman.2014.09.003.

397 Lockwood C.L., Stewart D.I., Mortimer R.J., Mayes W.M., Jarvis A.P., Gruiz K., Burke
398   I.T., 2015. Leaching of copper and nickel in soil-water systems contaminated by
399   bauxite residue (red mud) from Ajka, Hungary: The importance of soil organic
400   matter. Environ. Sci. Pollut. Res. 22, 10800-10810.
401   http://dx.doi.org/10.1007/s11356-015-4282-4.

402 Lu G., Chi S., Bi S., 2010. Leaching of alumina and iron oxide from red mud. J. Mater.
403   Metal., 31-34, 67. (in Chinese)

404 Mayes W.M., Burke I.T., Gomes H.I., Anton A.D., Molnar M., Feigl V., Ujaczki E.,
405   2016. Advances in understanding environmental risks of red mud after the Ajka
406   spill, Hungary. J. Sustain. Metal., 1-12. http://dx.doi.org/10.1007/s40831-016-
407   0050-z.

408 Menzies N.W., Fulton I.M., Morrell W.J., 2004. Seawater neutralization of alkaline
409   bauxite residue and implications for revegetation. J. Environ. Qual. 33, 1877-1884.
410   http://dx.doi.org/10.2134/jeq2004. 1877.

411 Power G., Gräfe M., Klauber C., 2011. Bauxite residue issues: I. Current management,
412   disposal   and   storage   practices.   Hydrometallurgy.   108,   33-45.
413   http://dx.doi.org/10.1016/j.hydromet.2011.02. 006.

414 Pulford I.D. et al., 2012. Carbonised red mud - a new water treatment product made
415   from   a   waste   material.   J.   Environ.   Manage.   100,   59-64.
416   http://dx.doi.org/10.1016/j.jenvman.2011.11.016.

417 Rai S.B., Wasewar K.L., Mishra R.S., Mahindran P., Chaddha M.J., Mukhopadhyay J.,
418   Yoo C., 2013. Sequestration of carbon dioxide in red mud. Desalin. Water Treat.
419   51, 2185-2192. http://dx.doi.org/ 10.1080/19443994.2012.734704.

420 Renforth P., Mayes W.M., Jarvis A.P., Burke I.T., Manning D.A.C., Gruiz K., 2012.
421   Contaminant mobility and carbon sequestration downstream of the Ajka (Hungary)
422   red mud spill: The effects of gypsum dosing. Sci. Total Environ. 421-422, 253-
423   259. http://dx.doi.org/10.1016/j.scitotenv. 2012.01.046.

424 Ruyters S., Mertens J., Vassilieva E., Dehandschutter B., Poffijn A., Smolders E., 2011.
425   The red mud accident in ajka (Hungary): Plant toxicity and trace metal
426   bioavailability in red mud contaminated soil. Environ. Sci. Technol. 45, 1616-
427   1622. http://dx.doi.org/10.1021/es104000m.

428 Sahu R.C., Patel R.K., Ray B.C., 2010. Neutralization of red mud using CO_2
429   sequestration   cycle.   J.   Hazard.   Mater.   179,   28-34.
430   http://dx.doi.org/10.1016/j.jhazmat.2010.02.052.

431 Samal S., Ray A.K., Bandopadhyay A., 2015. Characterization and microstructure
432   observation of sintered red mud-fly ash mixtures at various elevated temperature.
433   J. Clean. Prod. 101, 368-376. http://dx.doi.org/10.1016/j.jclepro.2015.04.010.

434 Santini T.C., Banning N.C., 2016. Alkaline tailings as novel soil forming substrates:
435   Reframing perspectives on mining and refining wastes. Hydrometallurgy. 164, 38-
436   47. http://dx.doi.org/ 10.1016/j.hydromet.2016.04.011.

437 Santini T.C., Fey M.V., 2015. Assessment of Technosol formation and in situ
438   remediation   in   capped   alkaline   tailings.   Catena.   136,   17-29.
439   http://dx.doi.org/10.1016/j.catena.2015.08.006.

440 Santini T., Fey M., Gilkes R., 2015. Experimental simulation of long term weathering
441   in   alkaline   bauxite   residue   tailings.   Metals.   5,   1241-1261.
442   http://dx.doi.org/10.3390/met5031241.

443 Si C., Ma Y., Lin C., 2013. Red mud as a carbon sink: Variability, affecting factors and
444   environmental   significance.   J.   Hazard.   Mater.   244-245,   54-59.
445   http://dx.doi.org/10.1016/j.jhazmat.2012.11.024.

446 Snars K., Gilkes R.J., 2009. Evaluation of bauxite residues (red muds) of different
447   origins   for   environmental   applications.   Appl.   Clay   Sci.   46,   13-20.

448   http://dx.doi.org/10.1016/j.clay.2009.06. 014.

449 Wang Q., Li J., Zhao Y., Luan Z., 2009. Study on the dealkalization of red mud by
450   suspension and carbonation. Chin. J. Environ. Eng. 3, 2275-2280. (in Chinese)

451 Wissmeier L., Barry D.A., Phillips I.R., 2011. Predictive hydrogeochemical modelling
452   of bauxite residue sand in field conditions. J. Hazard. Mater. 191, 306-324.
453   http://dx.doi.org/10.1016/j.jhazmat. 2011.04.078.

454 Xue S.G., Kong X.F., Zhu F., Hartley W., Li X.F., Li Y.W., 2016. Proposal for
455   management and alkalinity transformation of bauxite residue in China. Environ.
456   Sci. Pollut. Res. 23, 1-13. http://dx. doi.org/10.1007/s11356-016-6478-7.

457 Xue S.G., Zhu F., Kong X.F., Wu C., Huang L., Huang N., Hartley W., 2016. A review
458   of the characterization and revegetation of bauxite residues (Red mud). Environ.
459   Sci. Pollut. Res. 23, 1120-1132. http://dx.doi.org/10.1007/s11356-015-4558-8.

460 Yadav V.S., Prasad M., Khan J., Amritphale S.S., Singh M., Raju C.B., 2010.
461   Sequestration of carbon dioxide (CO_2) using red mud. J. Hazard. Mater. 176, 1044-
462   1050. http://dx.doi.org/10.1016/ j.jhazmat.2009.11.146.

463 Zhu F., Xue S.G., Hartley W., Huang L., Wu C., Li X.F., 2016b. Novel predictors of
464   soil genesis following natural weathering processes of bauxite residues. Environ.
465   Sci. Pollut. Res. 23, 2856-2863. http://dx.doi.org/10.1007/s11356-015-5537-9.

466 Zhu F., Zhou J.Y., Xue S.G., Hartley W., Wu C., Guo Y., 2016a. Aging of bauxite
467   residue in association of regeneration: A comparison of methods to determine
468   aggregate stability & erosion resistance. Ecol. Eng., 47-54.
469   http://dx.doi.org/10.1016/j.ecoleng.2016.03.025.

470 Zhu X.B., Li W., Guan X.M., 2015a. Kinetics of titanium leaching with citric acid in
471   sulfuric acid from red mud. T. Nonferr. Metal. Soc. 25, 3139-3145.
472   http://dx.doi.org/10.1016/S1003-6326(15) 63944-9.

473 Zhu X.B., Li W., Guan X.M., 2015b. An active dealkalization of red mud with roasting
474   and water leaching. J. Hazard. Mater. 286, 85-91.
475   http://dx.doi.org/10.1016/j.jhazmat.2014.12.048.

476